Research paper J. Electrochem. Sci. Technol. 7(1), 33-40 (2016)

Journal of Electrochemical Science and Technology

Characteristics of $Sr_{0.92}Y_{0.08}TiO_{3-\delta}$ Anode in Humidified Methane Fuel for Intermediate Temperature Solid Oxide Fuel Cells

Eun Kyung Park and Jeong Woo Yun*

School of Applied Chemical Engineering, Chonnam National University, Gwangju 500-757, Republic of Korea

ABSTRACT

$Sr_{0.92}Y_{0.08}TiO_{3-\delta}$ (SYT) was investigated as an alternative anode in humidified CH_4 fuel for SOFCs at low temperatures (650 °C-750 °C) and compared with the conventional Ni/yttria-stabilized zirconia (Ni/YSZ) anode. The goal of the study was to directly use a hydrocarbon fuel in a SOFC without a reforming process. The cell performance of the SYT anode was relatively low compared with that of the Ni/YSZ anode because of the poor electrochemical catalytic activity of SYT. In the presence of CH_4 fuel, however, the cell performance with the SYT anode decreased by 20%, in contrast to the 58% decrease in the case of the Ni/YSZ anode. The severe degradation of cell performance observed with the Ni/YSZ anode was caused by carbon deposition that resulted from methane thermal cracking. Carbon was much less detected in the SYT anode due to the catalytic oxidation. Otherwise, a significant amount of bulk carbon was detected in the Ni/YSZ anode.

Keywords : Solid oxide fuel cell, $Sr_{0.92}Y_{0.08}TiO_{3-\delta}$, methane, alternative anode, carbon deposition

Received 22 November 2015 : Revised 2 November 2015 : Accepted 3 November 2015

1. Introduction

Solid oxide fuel cells (SOFCs) are considered an attractive alternative conversion device because of their high efficiency and wide operating temperature range (800 °C-1000 °C). Fuel flexibility is one of the most significant advantages in SOFCs. Commercial hydrocarbons, such as natural gas, LPG, coal-gasified gas, and diesel, can be directly used as a fuel via internal reforming in SOFCs because of the relatively high operating temperatures [1,2]. This fuel flexibility minimizes the need for additional equipment, such as an external reformer and/or purifier, leading to improved overall system efficiency and lower operation costs. Nickel and yttria-stabilized zirconia (Ni/YSZ) cermet are most widely used as the anode material in SOFCs. Nickel provides good electronic conductivity and catalytic activity, while anodes containing YSZ provide good ionic conductivity and reduced thermal mismatch between the electrolyte and the anode. Ni/YSZ, however, cannot be selected as an SOFC anode for the direct use of commercial hydrocarbon fuels, because carbon may deposit on the bulk Ni surface, leading to a reduction in the cell performance. Carbon deposition could decrease the electrochemical performance of the cell by covering the triple phase boundary (TPB) where the electrochemical reaction occurs. Moreover, carbon deposition in anode pores could block the fuel gas stream, thereby increasing gas diffusion resistance [3,4]. The deposited carbon could diffuse into the bulk Ni phase, resulting in disruption of the anode structure.

*Corresponding author. Tel.: +82-62-530-1908
E-mail address: jwyun@jnu.ac.kr

Open Access DOI: http://dx.doi.org/10.5229/JECST.2016.7.1.33

Recently, much work has been devoted to developing Ni-free alternative anodes for the direct utilization of practical hydrocarbon fuels. These alternative SOFC anode materials must fulfill the following requirements [1,5]: (i) they must be electro-catalytically active for oxidation of the hydrocarbon fuel; (ii) the anodes must be both ionically and electronically conductive; (iii) they must be stable under reducing atmospheric conditions at high temperatures; (iv) they must be chemically compatible with the electrolyte; and (v) they must be resistant to carbon deposition and sulfur poisoning. Recently, various perovskite structure-based anodes have been reported to overcome these problems. Doped perovskite materials, such as doped strontium titanate [6-9] and doped lanthanum chromite [10-12], could be good candidates for alternative anode materials. These perovskite materials often show mixed ionic and electronic conductive (MIEC) properties, hence, the electrochemically active sites in the anode can be extended beyond the TPB area. The perovskite-base anode, however, has not sufficient electrochemical property as an alternative anode materials comparing to the Ni-based cermet.

In our previous study, we reported the use of yttria-doped strontium titanium oxide (SYT) as an alternative anode material [13,14]. SYT has good electronic conductivity in reducing conditions and stable chemical properties for hydrocarbon fuels. In this study, $Sr_{0.92}Y_{0.08}TiO_{3-\delta}$ was investigated as an alternative anode for CH_4 fuel in SOFCs at low temperatures (650 °C-750 °C).

2. Experiment

Strontium nitrate ($Sr(NO_3)_3$, Aldrich), yttrium nitrate hexahydrate ($Y(NO_3)_3 \cdot 6H_2O$, Aldrich), and titanium isopropoxide ($Ti[OCH(CH_3)_2]_4$, Junsei) were used to synthesize $Sr_{0.92}Y_{0.08}TiO_{3-\delta}$ (SYT) via the Pechini method. Strontium nitrate and yttrium nitrate hexahydrate were mixed in de-ionized water at 70 °C, and then citric acid ($C_6H_8O_7$) and ethylene glycol ($C_2H_6O_2$) were added to the solution. Titanium isopropoxide was solubilized in ethanol (99.9%). The two prepared solutions were mixed with NH_3OH at 70 °C for 5 h. A white-colored gel formed after drying at 150 °C for 24 h. The gel was burned at 600 °C for 10 h to form the SYT compound. The synthesized crystal structure was analyzed by an X-ray diffractometer (XRD, Rigaku, RINT-5200).

Electrolyte-supported single cells were prepared to investigate carbon deposition effects on the SYT anode. The electrolyte support was made by uniaxial pressurization (Carver Press Inc., USA) using a commercial 20 mol% gadolinium-doped powder sintered at 1400 °C for 6 h. The thickness and diameter of the GDC electrolyte were 1.0 mm and 25.0 mm, respectively. The anode was prepared by coating the SYT slurry on the electrolyte with a size of 0.69 cm^2 using the tape-casting method. After co-sintering the anode/electrolyte at 1400 °C for 10 h in air, $La_{0.85}Sr_{0.15}MnO_3$ (LSM) paste was coated on the GDC electrolyte as the cathode using the tape-casting method, and was fired at 1100 °C. The cathode and anode layers were about 30 μm thick. The microstructure of the SYT anode was analyzed using a scanning electron microscope (FE-SEM, Hitachi, S-4200, Japan) and an electro probe micro analyzer (FE-EPMA, JXA-8500F; JEOL, Japan).

The electrode characteristics were also measured using an impedance analysis device (SP-150, Biologic Science Instrument). The impedance spectra were recorded in the frequency range of 10^{-2}-10^6 Hz with an exciting voltage of 30 mV to ensure a linear response. Fig. 1 shows a schematic diagram of the reactor used to measure the cell performance. The cell was sealed with Pyrex glass on the anode side. A perforated Pt plate (1 cm^2 in area) and Pt wire (0.5 mm in diameter) were used as the current collector. In addition, the hydrogen, methane, and oxygen used in the experiments were humidified using a bub-

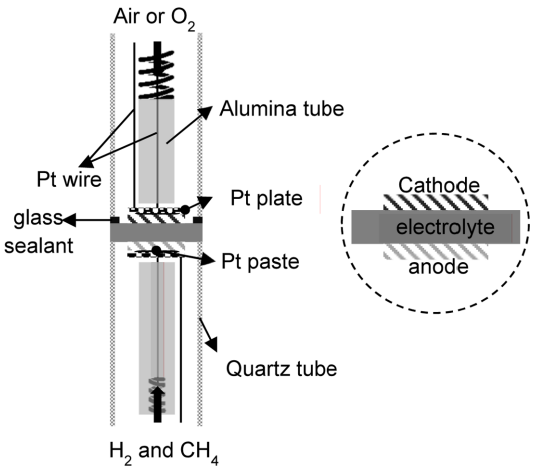

Fig. 1. Schematic diagram of the cell reactor.

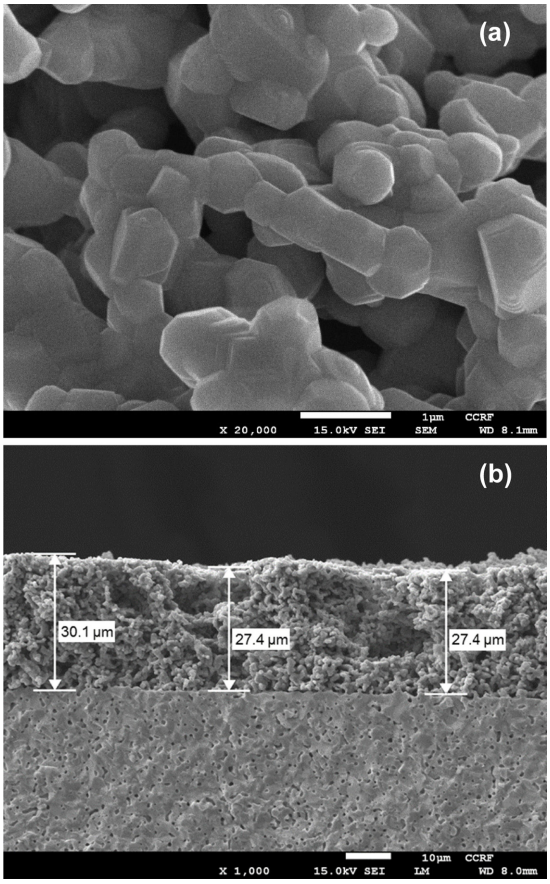

Fig. 2. Cut view of the SEM images used for nanostructure analysis of the SYT anode (a), and the interlayer between the SYT anode and GDC electrolyte(b).

bler at room temperature (25 °C). The gas flow rate was 200 mL/min in both cathode and anode.

3. Results and Discussion

Fig. 2 shows the cut view of the SEM images of the SYT anode (a), and the interlayer between the SYT anode and the GDC electrolyte (b). The anode porosity and average pore diameter after reducing in H_2 were ~40% and 3-5 μm, respectively. The SYT anode and the LSM cathode were uniformly formed with 30 μm thickness. Fig. 3(a) shows the XRD patterns of SYT (bottom), GDC (middle), and SYT/GDC composite (top). These patterns were used to investigate the chemical compatibility of the SYT anode with the GDC electrolyte. The SYT anode on the GDC electrolyte was co-sintered at 1400 °C to verify the byproduct formation between the anode and the electrolyte during the SOFC fabrication process. The SYT powder was mixed with GDC powder by dry ball milling, in a 50:50 weight ratio, for 10 h. After drying at room temperature, the SYT/GDC mixed powder was sintered at 1400 °C for 10 h in air. The XRD patterns of the SYT/GDC mixture were compared with those of SYT and GDC, which were also sintered at 1400 °C. No reaction byproducts were detected other than the SYT phase and the GDC phase. Doping yttria (Y_2O_3) into the strontium titanate ($SrTiO_3$) lattice can also be verified by small peak shifts as shown in Fig. 3(b). The first peak of SYT was slightly shifted compared with $SrTiO_3$ after dop-

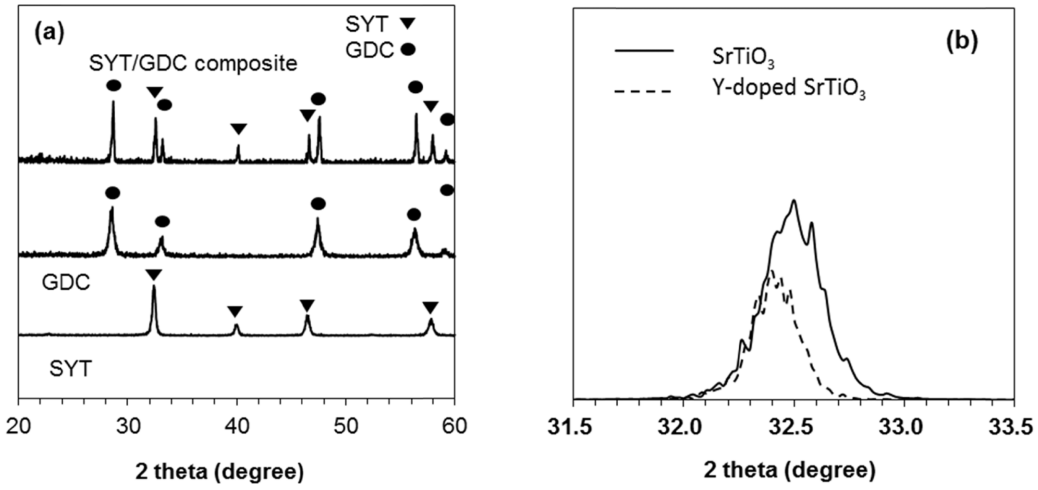

Fig. 3. XRD patterns of the GDC/SYT mixture: (a) After co-sintering at 1400 °C for 10 hr in air and (b) peak comparison of $SrTiO_3$ with Y-doped $SrTiO_3$.

ing yttrium ions into strontium ion sites.

Fig. 4 shows the electrical conductivity of SYT at 600 °C, 650 °C, 700 °C, 750 °C, and 800 °C in air, H_2, and CH_4 atmospheric conditions. SYT samples were prepared in rectangular bar shapes (31.7 × 8.9 × 8.4 mm), sintered at 1400 °C, and subjected to electrical conductivity measurements by a 4-point probe DC method. Under reducing conditions, the conductivities were 0.45, 0.59, and 0.81 S/cm in hydrogen, and 0.64, 0.88, and 1.25 S/cm in methane at 600 °C, 700 °C, and 800 °C, respectively. The electrical conductivity increased with increasing temperature, which corresponds to the conducting behavior in a ceramic material by a donor with Fermi level that is a function of temperature. The conductivity in CH_4 was higher than that in H_2. A thin carbon layer, being an electronic conductor, formed on the surface of the SYT anode by the thermal decomposition of CH_4. Under oxidizing conditions, the conductivity was 0.14, 0.22, and 0.43 S/cm at 600 °C, 700 °C, and 800 °C, respectively. The mismatch of charged valences between A and A' ions in the A-site-doped perovskite structure ($A_{1-x}A'_xBO_3$ structure) causes the electrical conductivity of Y doped-$SrTiO_3$. Sr^{2+} in $SrTiO_3$ may be substituted by Y^{3+} in Y_2O_3 (Eq. (1)) because the ionic radius of Y^{3+}(1.19 Å for twelve coordination) is smaller than that of Sr^{2+}(1.44 Å for twelve coordination). This substitution with a cation of different charge valence results in the formation of a lattice defect to maintain the electrical neutrality of the crystals.

$$Y_2O_3 \xrightarrow{SrO} 2Y_{Sr}^{\bullet} + 3O_O^X + V_{Sr} + 2e \quad (1)$$

Sr^{2+} cation lattices in $SrTiO_3$ are substituted with Y^{3+}. Strontium vacancies and 2 free electrons are also formed at the same time to maintain the electrical neutrality of the crystals, which acts as an n-type semiconductor. The reason for the different electrical conductivity values compared with our previous study could be differences in the porosity of the sample. Porosity differences could be caused by the different synthesis processes, such as heat treatment, sintering time, etc. [15-17].

Fig. 5 shows the impedance spectra of the SYT anode at various temperatures in humidified hydrogen. We prepared an SYT symmetric cell with a Pt reference electrode. The samples were evaluated under open circuit voltage (OCV) conditions. Impedance spectral data were obtained after 30 min, for stabilization. The polarization resistance of the SYT anode in humidified hydrogen was 4.25 Ωcm^2, 1.53 Ωcm^2, and 0.57 Ωcm^2 at 650 °C, 700 °C, and 750 °C, respectively. The polarization resistance decreased as the temperature increased. The electrical conductivity and electrochemical catalytic activity increased as the temperature increased.

Fig. 6 shows a comparison of the polarization resistance for (a) the SYT anode and (b) the Ni/YSZ anode in H_2 and CH_4 at 750 °C. The Ni/YSZ anode on a GDC electrolyte-supported cell was prepared under the same fabrication conditions as the SYT

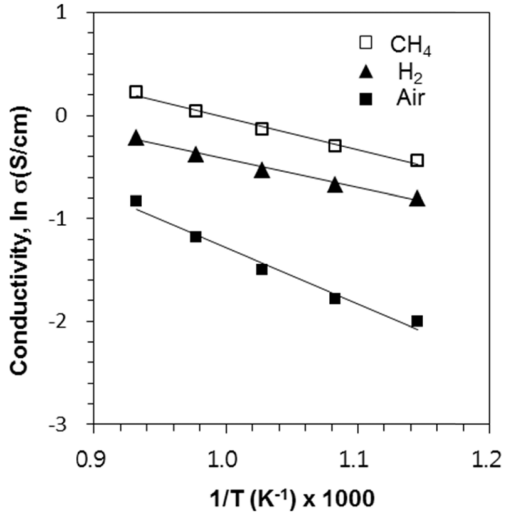

Fig. 4. SYT conductivity in air, H_2, and CH_4.

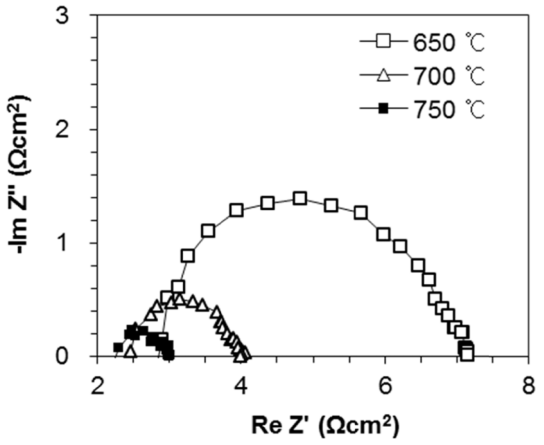

Fig. 5. Impedance spectra of half-cells with the SYT anode in humidified H_2 at 650 °C, 700 °C, and 750 °C.

anode to compare the anode resistance. In humidified methane fuel, the polarization resistance of the SYT anode slightly increased from 0.57 Ωcm^2 to 0.79 Ωcm^2, although the internal resistance (IR) increased from 2.26 Ωcm^2 to 2.69 Ωcm^2. The polarization resistance of the Ni/YSZ anode significantly increased from 0.47 Ωcm^2 to 1.36 Ωcm^2 in humidified CH_4. The electrochemical reaction may occur over the entire surface of SYT anode because the SYT has mixed electronic and ionic conductive (MIEC) properties in reducing conditions [18-20]. The anode polarization resistance of the SYT anode, however, was larger than that of the Ni/YSZ anode in H_2 conditions. The intrinsic catalytic activity of the SYT might be lower than that of Ni-based materials. In humidified CH_4, the anode polarization resistance of the SYT anode and the Ni/YSZ anode increased 38% and 280%, respectively. The carbon deposition could be the major cause of the significant increase of the polarization resistance in the Ni/YSZ anode. The SYT has only electronic conductivity via reaction mechanism equation(1) in oxidizing condition. However, the SYT($Sr_{0.92}Y_{0.08}TiO_{3-\delta}$) might have ionic conductivity in reducing condition as well as electronic conductivity, which it shows MIEC behavior. Therefore, electrochemical reaction could occur in entire anode surface(2D). Deposited carbon could be oxidized to CO or CO_2 via the electrochemical oxidation, which the mechanisms is given by,

$$C_{surface} + O^{2-} \rightarrow CO(g) + 2e \quad (2)$$

$$C_{surface} + 2O^{2-} \rightarrow CO_2(g) + 4e \quad (3)$$

where, the $C_{surface}$ refers to deposited carbon on the anode surface. Otherwise, the electrochemical reaction in the Ni/YSZ anode occurs in TPB area(3D) and the carbon formation likely occurs in the Ni phase. Therefore, the deposited carbon barely removed in the anode surface which results to major decrease of the cell performance. In our previous study, we reported that thermal decomposition of CH_4 fuel likely occurred in the Ni phase [4,21]. In addition, carbon deposition could cause major resistance in gas phase diffusion by blocking pores or decreasing pore size.

Fig. 7 shows the I-V characteristics of a single cell at varying temperatures (650 °C-750 °C) with a SYT

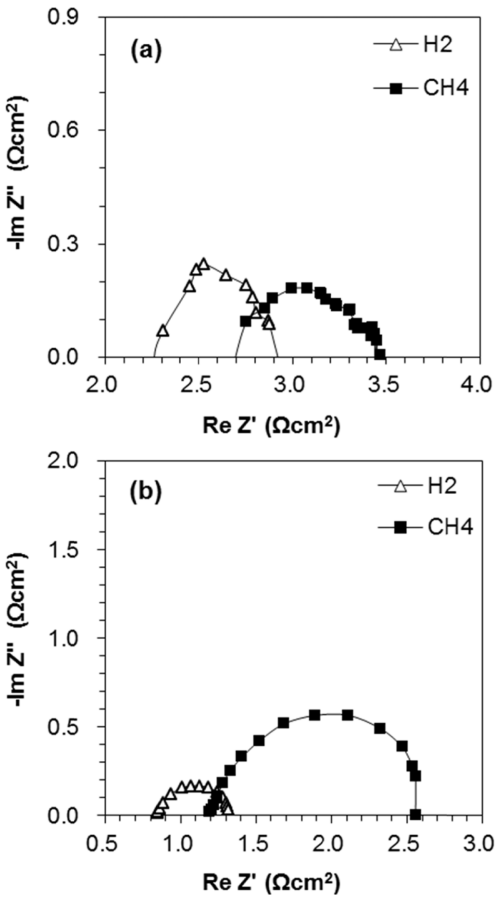

Fig. 6. Impedance spectra comparison in humidified H_2 and humidified CH_4 at 750 °C for (a) the SYT anode and (b) the Ni/YSZ anode.

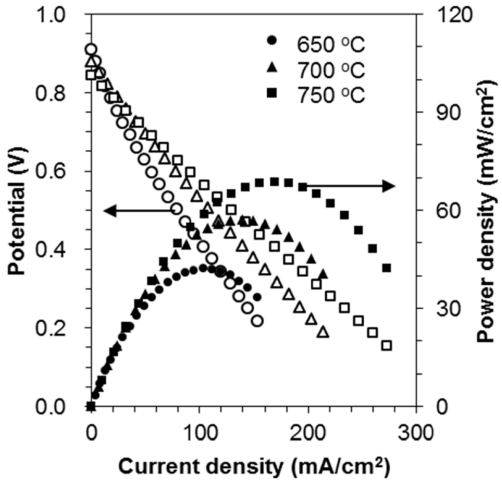

Fig. 7. I-V characteristics of the SYT anode cell in humidified H_2 at 650 °C, 700 °C, and 750 °C.

anode, GDC electrolyte (supporter), and LSM cathode. Gas flows of 200 mL/min for humidified H_2 (~3 vol% of H_2O) in the anode and excessive air in the cathode were used for the measurement of the I-V characteristics. The maximum power densities were 42.1 mW/cm^2, 57.1 mW/cm^2, and 68.8 mW/cm^2 at 650 ^{o}C, 700 ^{o}C, and 750 ^{o}C, respectively. The open circuit voltage (OCV) was ~0.9 V at every temperature, because GDC has electronic conductivity as well as a high ionic conductivity. A few electrons could be transferred through the GDC electrolyte leading to a decrease in OCV.

Fig. 8 shows a comparison of the cell performance at 750 ^{o}C for (a) the electrolyte-supported single cell with a SYT anode, and (b) a single cell with a Ni/YSZ anode. The GDC electrolyte and LSM cathode was used in the single cell fabrication. 200 mL/min of humidified H_2 (~3 vol% of H_2O) in the anode and excessive air in the cathode were used for measurement of the I-V characteristics. The maximum power density in the SYT anode was 68.6 mW/cm^2 and 55.1 mW/cm^2 in H_2 and CH_4 conditions, respectively. The maximum power density in the Ni/YSZ anode was 146.2 mW/cm^2 and 81.9 mW/cm^2 in H_2 and CH_4 conditions, respectively. Even though SYT has MIEC properties, the electrochemical catalytic activity is lower than Ni, leading to lower cell performance in the cell with the SYT anode. The performance of the cell with the SYT anode, however, decreased less than the cell with the Ni/YSZ anode in CH_4. In the presence of CH_4 gas in the anode, the cell performance with the Ni/YSZ anode decreased by 56 % in contrast to a 20 % decrease for the SYT anode. Even though methane could be electrochemically oxidized in the TPB sites, the pyrolysis of methane likely occurs in the Ni/YSZ anode. Carbon particles could deposit in the Ni phase leading to the deactivation of the TPB site and blocking of the anode pores. In addition, carbon could be deposited in the anode pores to form a bulk carbon phase, leading to blocking gas phase diffusion or decreasing pore size. Otherwise, since SYT has poor inherent catalytic activity for oxidation of CH_4, carbon deposition in the anode would be limited. The major merit of SYT anode comparing to the Ni/YSZ anode is utilization of direct hydrocarbon fuels. For the Ni/YSZ anode, the cell performance is much higher than that of the SYT anode at all temperature. The cell performance, however, is fatally decreased in hydrocarbon

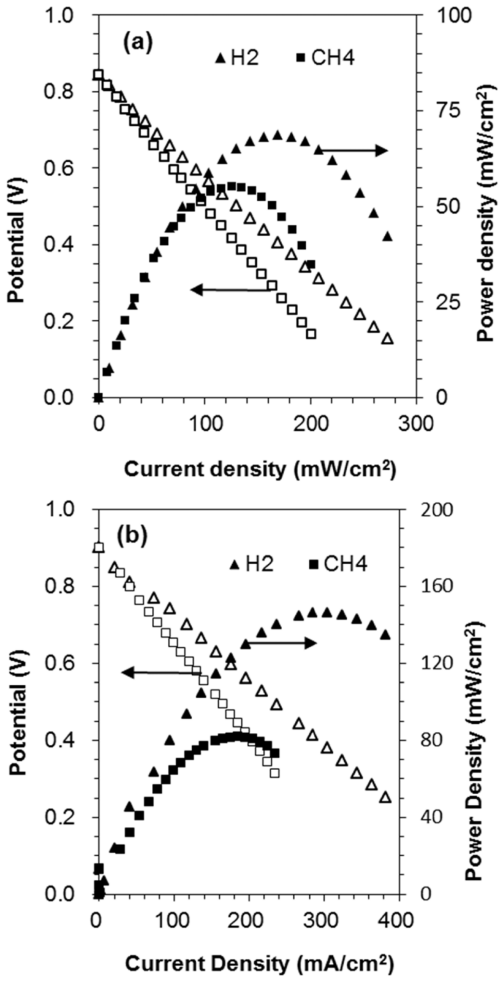

Fig. 8. Cell performance comparison of the SYT anode cell with the Ni/YSZ anode cell in humidified H_2 and humidified CH_4 at 750 ^{o}C.

fuel for long term operation. In our previous research, we reported the long term characteristics of the Ni/YSZ anode in CH4 fuel condition[21]. The cell performance of the Ni/YSZ anode was rapidly dropped within 60 hours to zero.

Fig. 9 shows EPMA mapping images of (a) the SYT anode surface and (b) the Ni/YSZ surface after operating 24 h in CH_4. After this time, the cell was quenched to room temperature in N_2 gas to analyze the carbon deposits on the anode surface. A significant amount of bulk carbon was detected on the Ni/YSZ anode. Less carbon was detected on the SYT anode. Based on the EPMA results, these carbon formations confirm that degradation of the cell perfor-

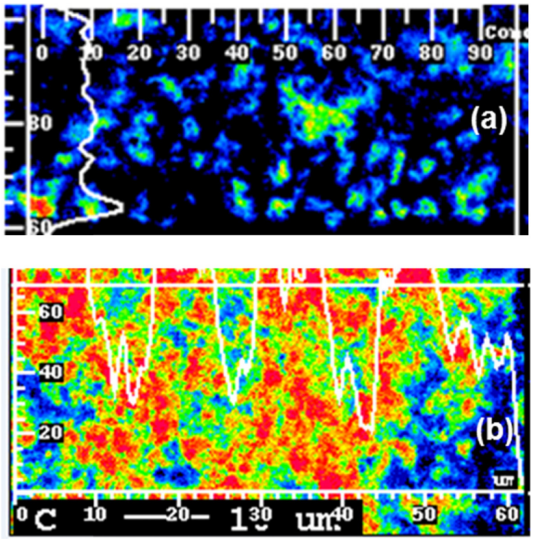

Fig. 9. Concentrations of carbon deposits from electro probe micro analyzer (EPMA) mapping of the surface of (a) the YST anode and (b) the Ni/YSZ anode.

mance shown in Fig. 6 and Fig. 8 directly affects cell performance. In addition, the bulk carbon formation shown in Fig. 9 could block the anode, which may lead to an increase of gas phase diffusion resistance.

4. Conclusion

$Sr_{0.92}Y_{0.08}TiO_{3-\delta}$ (SYT) was investigated as an alternative anode material so that hydrocarbon fuel could be used without a reforming process. A GDC electrolyte-supported cell with LSM cathode was prepared to investigate cell performance. The SYT anode was chemically stable with the GDC electrolyte. No reaction byproducts were detected other than the SYT phase and the GDC phase. Doping yttria (Y_2O_3) in the strontium titanate ($SrTiO_3$) lattice was confirmed by peak shifts in the XRD analysis. The conductivities of the SYT sample in reducing conditions were 0.45, 0.59, and 0.81 S/cm in hydrogen, and 0.64, 0.88, and 1.25 S/cm in methane conditions at 600ºC, 700 ºC, and 800 ºC, respectively. The polarization resistance of the SYT anode in humidified hydrogen was 4.25 Ωcm^2, 1.53 Ωcm^2, and 0.57 Ωcm^2 at 650 ºC, 700 ºC, and 750 ºC, respectively. In humidified CH_4, the anode polarization resistance of the SYT anode and the Ni/YSZ anode increased 38 % and 280 %, respectively. The cell performance with the Ni/YSZ anode decreased to 56 % of its original value. In the SYT anode, the cell performance decreased by only 20 %. Carbon deposition could be the major cause of the significant performance degradation in the Ni/YSZ anode. The EPMA results confirm that carbon formation on the anode affected the cell performance directly. In addition, bulk carbon formation could block the anode, which may lead to an increase in the resistance to gas phase diffusion.

Acknowledgement

This research was supported by Basic Science Research Program through National Research Foundation of Korea (NRF) funded by the Ministry of Education (NRF-2014R1A1A2056222)

References

[1] A. Atkinson, S. Barnett, R. J. Gorte, J. T. S. Irvine, A. J. McEvoy, M. Mogensen, S. C. Singhal and J. Vohs, *Nature mater.*, **3**, 17 (2004).
[2] R. M. Ormerod, *Chem. Soc. Rev.*, **32**, 17 (2003).
[3] K. Huang and J. B. Goodenough, *Solid oxide fuel cell technology: Principles, Performance and Operations*, Elesevier (2009).
[4] J. M. Lee, Y. G. Kim, S. J. Lee, H. S. Kim, S. P. Yoon, S. W. Nam, S. D. Yoon and J. W. Yun, *J. Appl. Electrochem.*, **44**, 581 (2014).
[5] J. B. Goodenough and Y.-H. Huang, *J. Power Sources,* **173**, 1 (2007).
[6] S. Hui and A. Petric, *J. European Ceramic Society,* **22**, 1673 (2002).
[7] X. Huang, H. Zhao, W. Shen, W. Qiu and W. Wu, *J. Physics and Chemistry of Solids,* **67**, 2609 (2006).
[8] S. Hui and A. Petric, *J. Electrochem. Soc.* **149**(1), J1 (2002).
[9] V. Vasechko, B. Huang, Q. Ma, F. Tietz and J. Malzbender, *J. Eur. Ceram. Soc.*, **34**, 3749 (2014).
[10] G. Xiao and F. Chen, *Frontiers in Energy research,* **2**(18), 1 (2014).
[11] N. Sakai, T. Kawada, H. Yokokawa, M. Dokiya and T. Iwata, *J. Mater. Sci.*, **25**, 4531 (1990).
[12] M. Mori and N. M Sammes, *Solid State Ionics,* **146**, 301 (2002).
[13] H. S. Kim, S. P. Yoon, J. W. Yun, S. A. Song, S.-C. Jang, S. W. Nam and Y.-G. Shul, *International Journal of hydrogen energy,* **37**, 16130 (2012).
[14] H. S. Kim, G. S. Kim, J. W. Yun, H. C. Ham, J. H. Jang, J. H. Han, S. W. Nam, Y.-G. Shul and S. P. Yoon, *Ceramics International*, **40**, 8237 (2014).
[15] Q. X. Fu, S. B. Mi, E. Wessel and F. Tietz, *J. Eur. Ceram. Soc.*, **28**, 811 (2008).
[16] M. García-Gabaldóna, V. Pérez-Herranz, E. Sánchezb

and S. Mestre , *J. Memb. Sci.,* **280**, 536 (2006).
[17] M. Y. Yoon, R.-H. Song, D.-R. Shin and H. J. Hwang, *J. Korean Powder Metall. Inst.,* **17**(1), 59 (2010).
[18] Q. Fu, F. Tietz, D. Sebold, S. Tao and J. T. S. Irvine, *J. Power Sources*, **171**, 663 (2007).
[19] H. He, Y. Huang, J. M. Vohs and R. J. Gorte, *Solid State Ionics*, **175**, 171 (2004).
[20] J. W. Yun, H. C. Ham, H. S. Kim, S. A. Song, S. W. Nam and S. P. Yoon, *J. Electrochem. Soc.*, **160**, F153 (2013).
[21] J. M. Lee, Y. G. Kim, S. J. Lee, H. S. Kim, S. P. Yoon, S. W. Nam, S. D. Yoon and J. W. Yun, *J. Appl. Electrochem*, **44**, 581 (2014)